

Nonlinear Analysis for Dynamics of Ferric Oxide (Fe_3O_4) Nanoparticles

Rashmi Bhardwaj and Aashima Bangia

University School of Basic and Applied Sciences

GGs Indraprastha University, Delhi-110078

Corresponding Author Email: rashmib@ipu.ac.in

(Received January 25, 2022)

Abstract: In the present study, the analysis of the ferro-nanofluidic flow for magnetic and temperature variability with magnetite (Fe_3O_4) nanoparticles through blood vessels along with cholesterol decomposition in cylindrical cavity system is studied. Nonlinear analysis using time series analysis, phase space analysis discussed. Lyapunov Indicators in this study compute regulated and chaotic motions of the non-linearity. Fixed points have been simulated and stable, critical and chaotic states are observed for non-uniform-deposition of cholesterol. Lyapunov Exponents and Bifurcation analysis also carried out for variation in Hartman number (H) and Reynold number (R). Entropy quantifies the probability of haphazardness in the dynamism. It can be concluded that for non-uniform cholesterol-deposition, R is high in value for the chaotic behaviour. Thus, patient with non-uniform cholesterol deposition has better chance of survival as randomness happens at risky conditions and due to non-uniformity of deposition there exist narrow passages which provide stable flow.

Keywords: Ferro-nanofluid, Bifurcation, Dynamic Lyapunov Indicators (DLI), Fast Lyapunov Indicators (FLI), Small Alignment Index (SALI), Entropy, Time series Analysis, Phase space analysis, Lyapunov Characteristic Exponent (LCE).

2010 AMS Subject Classification: 00A71-93A30.

1. Introduction

In enriched magnetic drug delivery, the super-paramagnetic iron oxide nanoparticles have been used being paramagnetic in nature and iron oxide (Fe_3O_4) nano-fluid has the particles oriented in random way in agreement to their individual spin which should to get oriented in drug delivery. In this paper, the fluid underlying-forces of ferro nano-fluidic flow with magnetite (Fe_3O_4) nanoparticles via blood-vessels along cholesterol-decomposition is

mathematically modelled in cylindrical cavity non-uniformly and variation of Hartman number. The horizontal fluid-layer forming the flow whenever exposed towards the heat as well as magnetic interaction with the parameter of gravity. Non-linear partial differential equations for mathematical model are developed using the equations overriding mass-conservation, momentum, energy & electric-charge transmission towards laminar flow with magnetic flux. It is a well-established fact that properties of material at nanoscale are quite different from the properties of the same material in bulk form. Nanoparticles possess quite unique optical, magnetic, electronic and catalytic properties. The increased interest in exploring the biomedical applications of nanoparticles arise from the fact that these can quite readily interact with biological system; these can easily enter a living organism either by inhalation, ingestion or by absorption through skin. The size domain of these particles allows them to easily pass through the biological membrane barriers as well as olfactory mucosa and can therefore readily enter the biological cell. This makes these materials very important as potential drug carriers, however, the toxicological profile also needs to be ascertained prior their use in applications involving living organisms. The nano-magnetite although well known for its electrical and magnetic properties, also finds tremendous biomedical applications. These include their use in: magnetic drug targeting, magnetic drug and gene delivery.

Hyperthermia is a state of increased body temperature due to some disease. An extreme increase in temperature many result in some disability or even death. The nano magnetite is used in site specific delivery for the treatment of hyperthermia. As for the above-mentioned purposes, the nano-magnetite suspensions are injected in biological system and are guided to desired site by means of powerful electromagnets. The suspension of iron oxide in a liquid is called ferrofluid. This fluid has a unique property that it can act as a magnetic solid as well as liquid. In the presence of a magnetic field the magnetite particles in the fluid are magnetized and enact as a solid while in absence of magnetic-field, these act as particles suspended in liquid. The radii of the magnetite particles range from 2-10 nm and this size range is responsible for uniform magnetization.

Advancements in non-linear physical systems provide certain newer methodologies such as FLI, SALI, DLI, etc. for understanding chaotic behavior. Characterizations of the indicators are: FLI escalates exponentially in case of chaotic behavior whereas linearly in case of regularity; SALI swings around the non-zero values for regular motions whereas converges to zero for chaotic ones; DLI are computed as the largest eigenvalues that designate a clear outline when the system has regular motion and are

generated randomly to show chaotic behavior. Bifurcation transpires at an instant where small smooth alteration is made to the factors of the system which in turn sources a sudden topological variation in their conduct. Entropy is a quantification of probability of the arbitrariness of the structure macroscopically. Bhardwaj *et al*¹⁻⁹ discussed the Fe₃O₄ nanoparticles in blood fluidic flow dynamics, control system through hybrid fuzzified PID controllers for nonlinearity in control surfaces, predicted atmospheric pollutants through indicators, complexities of meditating body dynamics, studied demonetization using soft computing, statistical analysis of HIV dynamics, neurofuzzy analysis of demonetization on NSE, explained malwares in IoT-based wireless transmissions, forecasted rainfall and temperature trends. Karami *et al*¹⁰ discussed a novel approach to be used for Fe₃O₄ nanoparticles as the magnetic recovery based catalyst. Nasr-Esfahani *et al*¹¹ studied magnetic nanoparticles as recoverable nanocatalyst under solvent-free conditions for synthesis. Khodabakhshia *et al*¹² explored the Fe₃O₄ nanoparticles as extremely efficient as well as recyclable catalyst for synthesis of 4-Hydroxy-3-[aryloyl(benzamido)methyl]coumarin. Lee *et al*¹³ captured the nanostructured sorbents in combustion environments. Kamat & Meisel¹⁴ explored the nanoscience application in the environment. Cuenca *et al*¹⁵ published the implications of nano in cancer diagnosis and perhaps treatment. Oberdörster *et al*¹⁶ studied nanotoxicology as an emerging study of ultrafine particles. Faraji *et al*¹⁷ described the application of nanoparticles in drug delivery systems. McBain *et al*¹⁸ employed these nanoparticles for gene study. Gupta & Gupta¹⁹ explored the cytotoxicity suppression and cell based enhancements for the surfaces through these nano. Gould²⁰ explained nanomagnetism in depth. Goya *et al*²¹ studied the static as well as dynamical magnetism characteristics for these particles. Gupta & Gupta²² synthesized and engineered the iron oxide nanoparticles in biomedical area. Buman & King²³ studied the exercise routine as an enhancement towards sleep. Buskirk & Jeffries²⁴ observed the randomness in coupling oscillators. Froeschle *et al*²⁵ presented the FLI technique to check upon the weak chaos in the systems.

2. Methodology

2.1. Dynamic Lyapunov Indicator (DLI):

Theorem 2.1: *DLI determine pattern recognized through largest eigenvalues.*

Remark 2.1: Let Jacobian matrix for the dynamical system be referred to as J . Then, at each discretized time-step, estimation of the eigenvalues of the matrix, J graphing that largest eigenvalue.

Remark 2.2: Eigenvalues in matrix formed by J can be simulated through:

$$J - \lambda_j I = 0$$

as per I - identity matrix; J - Jacobian matrix

Remark 2.3: These computed eigenvalues can be organized as a certain arrangement; motion is said to be regulated while the ones generating arbitrarily denote that the motion is going to be unpredictable.

2.2 Fast Lyapunov Indicator (FLI):

Theorem 2.2: *FLI is referred as largest value of eigenvector computed for every iterative step. This indicator is developed to reduce the dependency on the preliminary conditions.*

Remark 2.4: FLI calculated as:

$$FLI = \sup \|v_j\|, j=1:1:m$$

having v_j - m -dimensional basis for eigenvector.

Remark 2.5: Norm of a deviation vector diverges hastily to altogether extremely diverse values for two states: regular and chaotic.

Note: FLIs are clearly distinguishable between regular as well as chaotic behavior. FLI increases exponentially for random orbits but linearly for steady-ones.

2.3 Small Alignment Index (SALI):

Theorem 2.3: *SALI is designed to unmistakably determine the type of motion that system follows at each time evolution.*

Algorithm for computation of SALI:

1. Begin with the idea that there exists an n -dimensional phase-space of the system. Further, let there be an orbit having initial conditions (ICs): $P(0) = (x_1(0), x_2(0), \dots, x_n(0))$.
2. Then, deviance vector $\xi(0) = (dx_1(0), dx_2(0), \dots, dx_n(0))$ chosen at $P(0)$.

3. Now, monitor the time-evolution with respect to $P(0)$ having two deviance vectors $\xi_1(t), \xi_2(t)$ are not pointing the same directions at the beginning.
4. Evolution for deviance vectors as computed by variational-equations associated with the flow plus tangent-map for the case of discrete-time system.
5. Taking two deviance-vectors &, have to be standardized for every discretized time step so, the computation involves:

$$SALI(t) = \min \left\{ \left\| \frac{\xi_1(t)}{\|\xi_1(t)\|} + \frac{\xi_2(t)}{\|\xi_2(t)\|} \right\|, \left\| \frac{\xi_1(t)}{\|\xi_1(t)\|} - \frac{\xi_2(t)}{\|\xi_2(t)\|} \right\| \right\}$$

In case for n -dimensional, $n > 2$, it dithers around non-zero value in case of regulated motions. It converges towards zero for random motions. An exception for the case of 2D map states that SALI gradients towards zero for regulated and arbitrary ones, but with totally variant time-rates, to decide between the two cases.

2.4 Entropy:

Definition: The necessary assessment to be determined for the existing uncertainty that can alter or have the nearest possibility to alter the physical struct of the system can be termed as the *Entropy* of that system.

Note 1: Quite commonly at macroscopic level, entropy is simply taken to be the probability of the disarrangement of the existing structure.

A system having many variables to describe various factors taken into considerations. Mathematically, an intangible definition is involved for a better understanding of the concept.

Note 2: Consider a variable G . Then, entropy for G in a structure can be determined through:

$$\hbar(G) = -\sum_x p(g) \log_2 [p(g)] \text{ bits,}$$

$p(g)$ denotes probability of \hbar being in state g ; $p(\log_2 p)$ should be taken as zero as and when p equates zero.

Remark 2.6: Thus, combined entropy of G_1, \dots, G_n can be represented via:

$$\hbar(G_1, \dots, G_n) \equiv -\sum_{x_1} \dots \sum_{x_n} p(g_1, \dots, g_n) \log_2 [p(g_1, \dots, g_n)] \text{ bits,}$$

denotes $p(g_1, \dots, g_n)$: probability of \hbar being in state (g_1, \dots, g_n) .

3. Mathematical Modelling

Let us consider an infinitesimal blood vessel cavity through which iron oxide ferro nanofluid passes away having ultra-small super paramagnetic iron (ferrous/ferric) oxide nanoparticles referred as USPIO, iron oxide nanoparticles (IONPs), magnetic nanoparticles (MNPs). The fact that blood is Non-Newtonian in nature is considered to be not impacting the Newtonian nature of the nano-fluid as blood readily rejects MNPs which are generally remain dispersed in blood and even the aggregates formed by them are eventually removed by blood stream. The cholesterol deposition in the blood vessel is in two forms either uniform deposition or non-uniform in which case two kinds of cavity can be considered to be available for the nano-fluid to flow with blood as shown in Fig.4. Two elongated walls have been sustained at temp. T_H & T_C , respectively, while undersized end walls have been thermally-insulated. Vertically, z is collinear with gravity which means $\hat{e}_g = -\hat{e}_z$ and uniform. The fluid experiences mechanism behind buoyancy as discussed via Garandet. Fluid density alters through variation of temperature happening due to heat-transfers and the interacting environments containing magnetic field through the convective-motion. Reynolds number considered as insignificant, implying magnetic-field induced as insignificant.

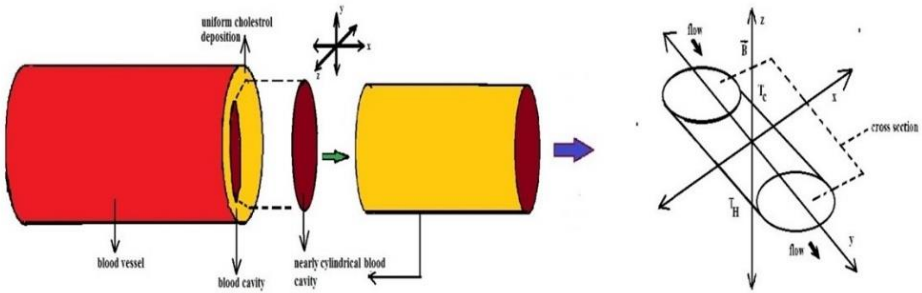


Figure 1: Cylindrical cavity type in the blood vessel having Cholesterol deposition

These calculations in detail can be referred to R. Bhardwaj and M. Chawla¹. Now, the reduced system analogous to Lorenz system can be expressed as:

$$\begin{aligned}\dot{X} &= \frac{dX}{d\tau} = \text{Pr} \bar{\nu} L [Y - X] \\ \dot{Y} &= \frac{dY}{d\tau} = TX - FY - MXZ \\ \dot{Z} &= \frac{dZ}{dt} = \bar{\alpha} \lambda [XY - Z]\end{aligned}$$

where

$$L = \frac{(r^2\pi^2 - 8)\pi^2}{(r^2\pi^2 - 4)} + \frac{\bar{\gamma}}{\bar{\nu}}$$

$$F = \frac{\bar{\alpha}(r^2\pi^2 - 1)}{r^2(r^2\pi^2 - 4)}$$

$$T = \frac{\bar{R}\bar{\varepsilon}}{\bar{\nu}L}$$

$$M = (T - F)\pi$$

$$\lambda = \frac{4\pi}{(r^2\pi^2 - 4)}$$

Thus, the governing equation for both the cases are obtained as partial differential equations through conservation of momentum & energy that can be represented as 3D nonlinear differential system which in dynamics is similar to Lorenz equations.

Now, system can be reduced as:

$$\dot{X} = c(Y - X) = f(X, Y, Z)$$

$$\dot{Y} = TX - FY - MXZ = g(X, Y, Z)$$

$$\dot{Z} = s(XY - Z) = h(X, Y, Z)$$

Consider

$$Pr = p;$$

$$\bar{\alpha} = a;$$

$$\bar{\nu} = v;$$

$$\bar{\varepsilon} = b;$$

$$\pi = d;$$

$$s = \bar{\alpha}\lambda = a\lambda;$$

$$L = \frac{(r^2\pi^2 - 8)\pi^2}{(r^2\pi^2 - 4)} + \frac{\bar{\gamma}}{\bar{\nu}}$$

$$F = \frac{\bar{\alpha}(r^2\pi^2 - 1)}{r^2(r^2\pi^2 - 4)}$$

$$T = \frac{R\bar{\epsilon}}{\bar{\nu}L}$$

$$M = (T - F)\pi$$

$$\lambda = \frac{4\pi}{(r^2\pi^2 - 4)}$$

4. Results and Discussions

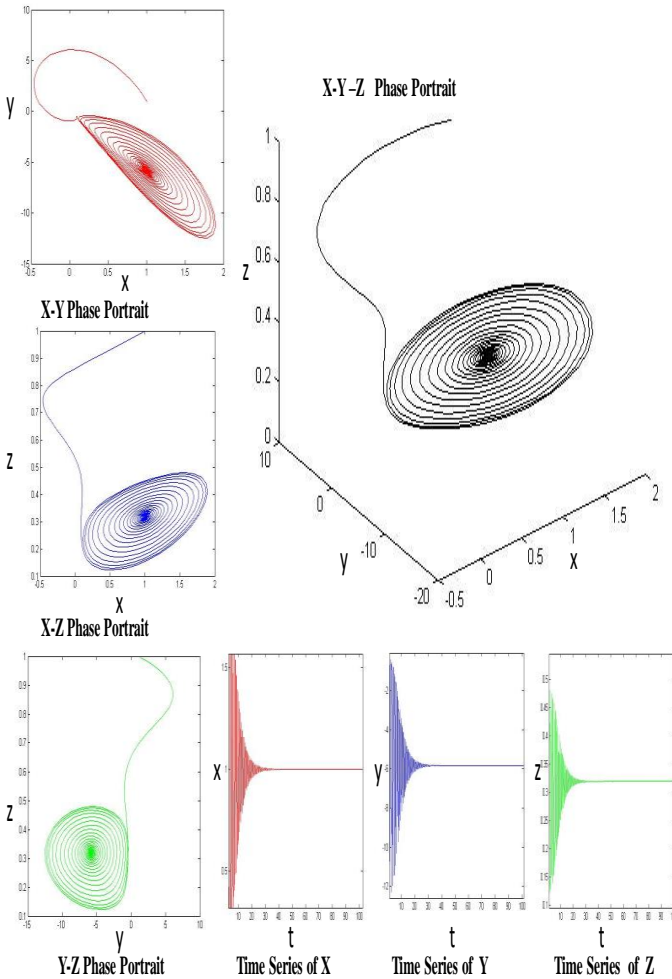


Figure 2: Phase portraits and Time series in cylindrical cavity for Pr=10, Ha=0.5 & Ra=21

To describe the dynamics of iron oxide nano-fluid with effect of magnetic field, the system of equations is arithmetically solved. The observed stages at different values of Hartmann number are shown through phase portraits and time series graphs. Figures 2, 3, 4, 5 and 6 towards the flow into cylindrical cavity when both Rayleigh and Hartman are varying at Pr =10.

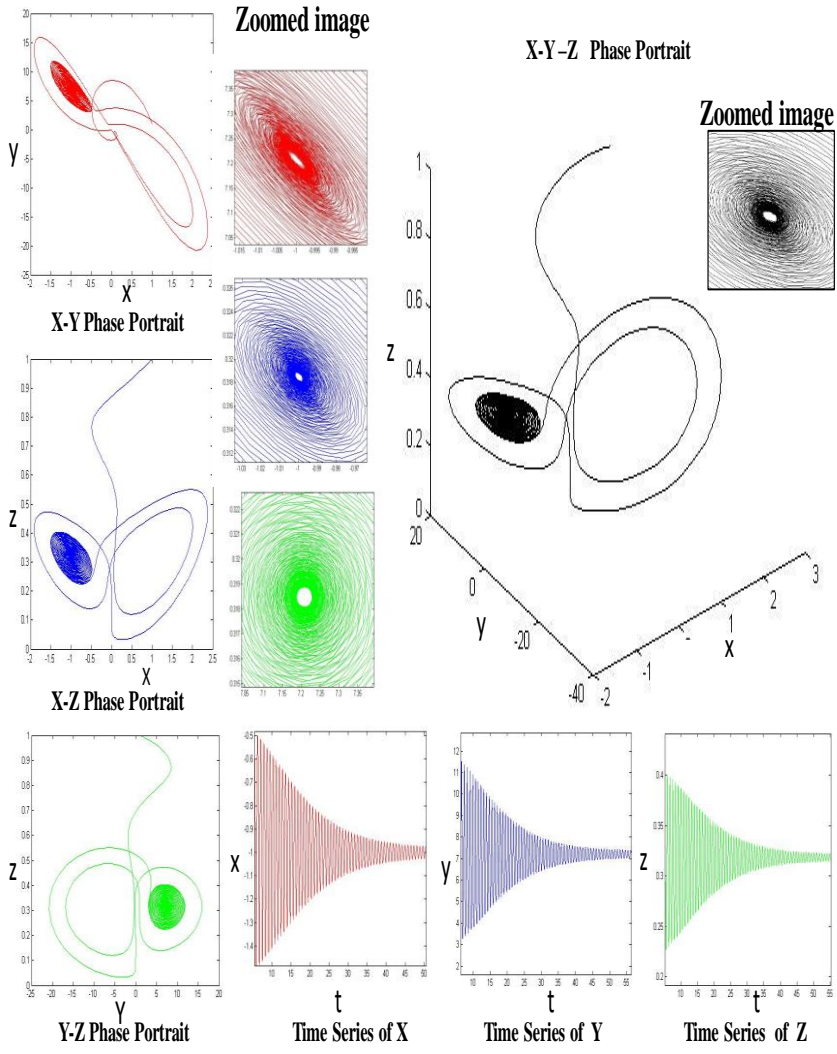


Fig 3: Phase portraits and Time series in cylindrical cavity for Pr=10, Ha=0.5 & Ra=25.7

The phase portrait obtained for the Fe₃O₄ convection for different values of Hartmann number variation verify the concept of using iron oxide fluids for channelized drug delivery and MRI contrast agent. When Rayleigh number is high during chaotic state then by increasing Hartman number stability in the convective flow of the iron oxide ferro-nanofluid in both cases is

obtained. DLI graphs are given in fig. 7(a), (b), (c). FLI graphs are given in fig. 8(a), (b), (c). SALI graphs are given in fig 9(a), (b), (c). Table 1 and 2 relate the values of Lyapunov Exponents with the change in Entropy showing their effect on stability of the system for different Rayleigh number (Ra) and different Hartmann number (Ha) respectively.

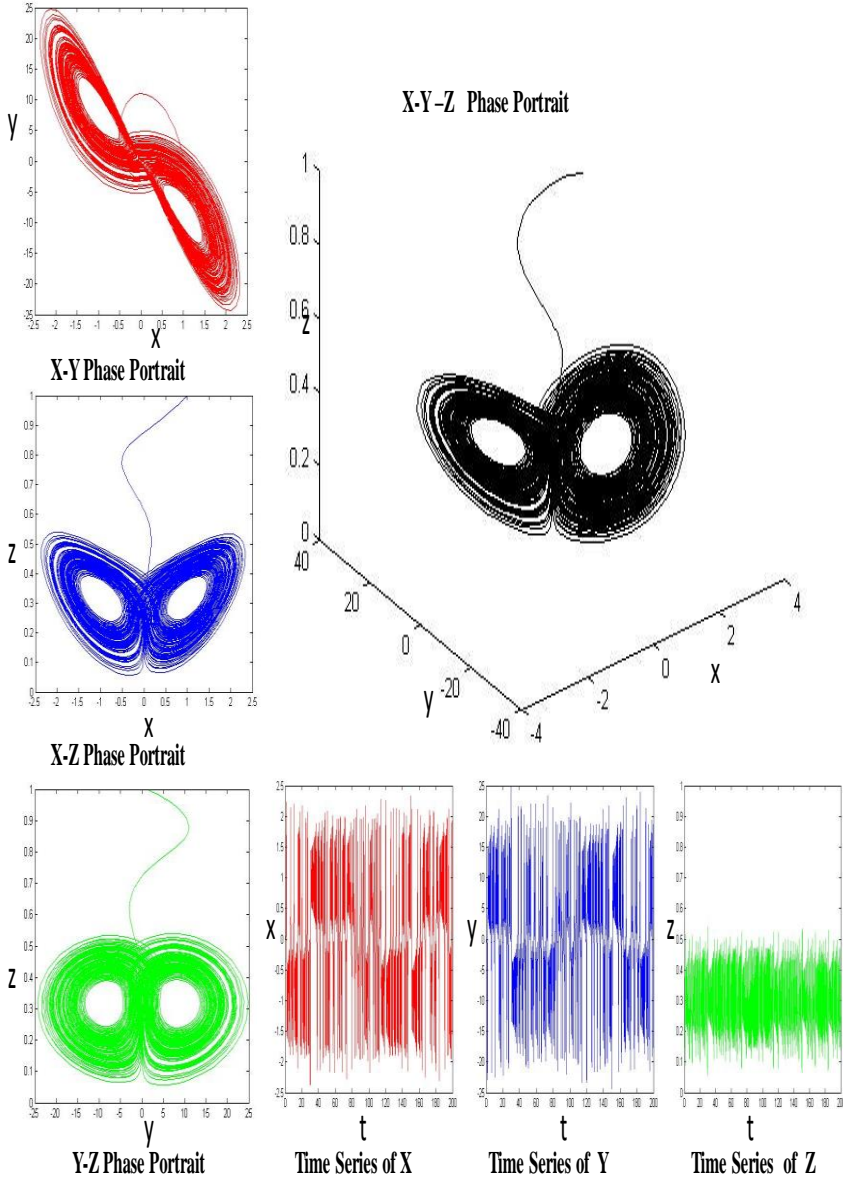


Figure 4: Phase portraits and Time series in cylindrical cavity for $Pr=10$, $Ha=0.5$ & $Ra=30$

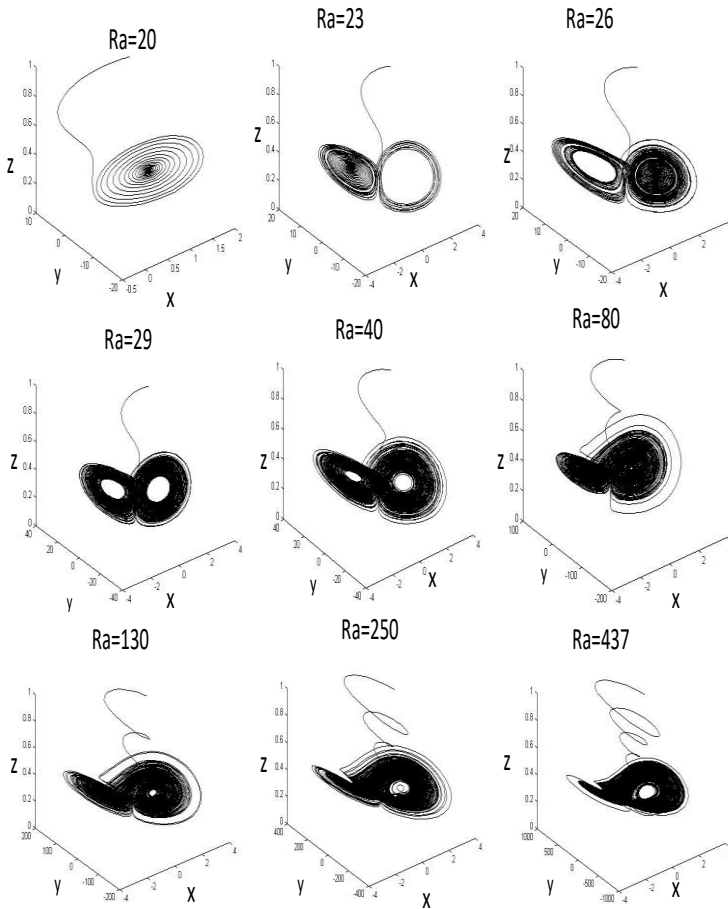


Fig 5: Transitions in Phase portraits in cylindrical cavity for Pr=10, Ha=0.5 & different Ra

Table-1: LCE and Entropy value showing stability change for Ha= 0.5 and different Rayleigh number(Ra)

Values of Ra	λ_1	λ_2	λ_3	Entropy (H)	Stability changes
20	-1.830000	-6.334287	-22.438286	3.04603	Stable
25	0.0	-4.816987	-25.754379	3.5406	Critical
28	0.096901	-3.600364	-27.099110	4.9250	Chaotic
35	0.683552	0.121545	-14.903514	4.9637	Hyper Chaotic
50	0.587698	-0.326808	-15.580508	4.6865	Strange Chaotic
100	0.503411	-0.203859	-15.619169	4.5554	Strange Chaotic
120	0.745520	-0.244495	-14.842533	4.5270	Chaotic
150	0.739989	-0.214295	-14.867202	4.5510	Chaotic
180	0.727438	-0.204399	-14.864547	4.5039	Chaotic
200	0.619552	-0.132196	-14.828864	4.5237	Chaotic

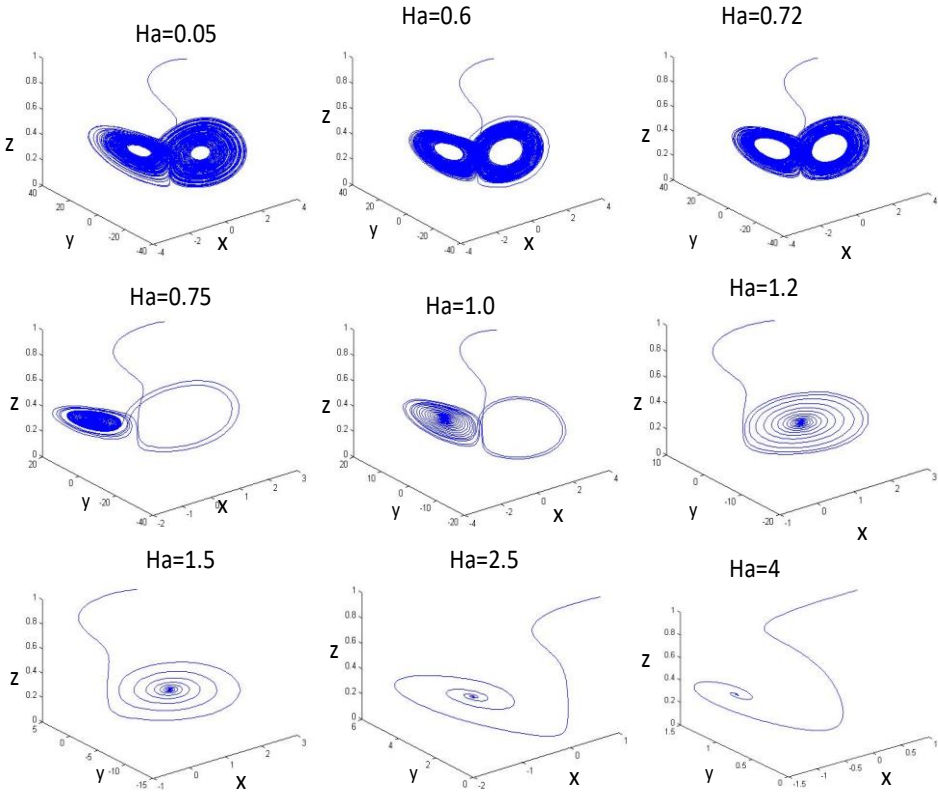


Fig 6: Transitions in Phase portraits in cylindrical cavity for $Pr=10$, $Ra=30$ & different Ha

Table-2: LCE and Entropy value showing stability change for $Ra=28$ and different Hartmann number

Values of Ra	λ_1	λ_2	λ_3	Entropy (H)	Stability changes
0.1	1.068814	-1.430689	-13.972100	4.8823	Strange Chaotic
0.2	0.419493	0.755823	-13.996932	4.9503	Hyper chaotic
0.5	0.333029	0.658461	-14.007491	4.9637	Hyper chaotic
0.7	0.356355	0.487138	-14.201877	4.9510	Hyper chaotic
1.0	0.0	-1.918074	-28.021816	3.0475	Critical
1.2	0.0	-1.775615	-28.087586	2.5748	Critical
1.5	0.0	-1.879627	-28.170574	2.3082	Critical
1.7	-0.556427	-1.809923	-28.236223	2.2441	Stable
2.0	-0.650748	-1.667605	-28.284220	1.9978	Stable
2.5	-0.881354	-1.387722	-28.333498	1.9218	Stable

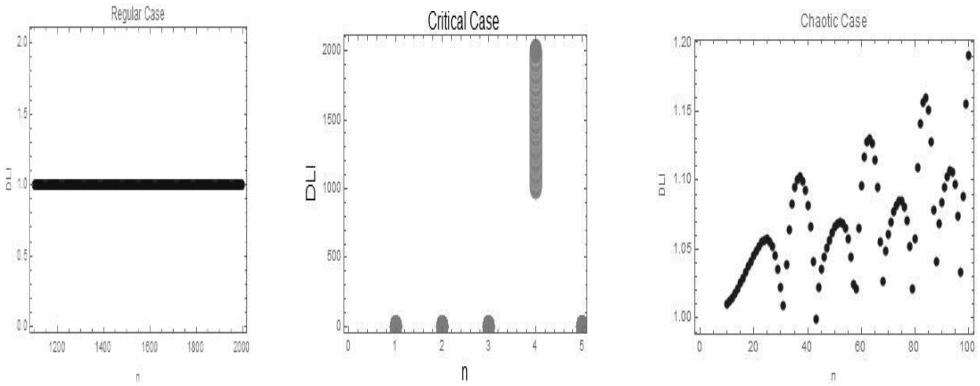


Fig. 7(a). DLI for regular case (b). DLI for critical case (c). DLI for chaotic case

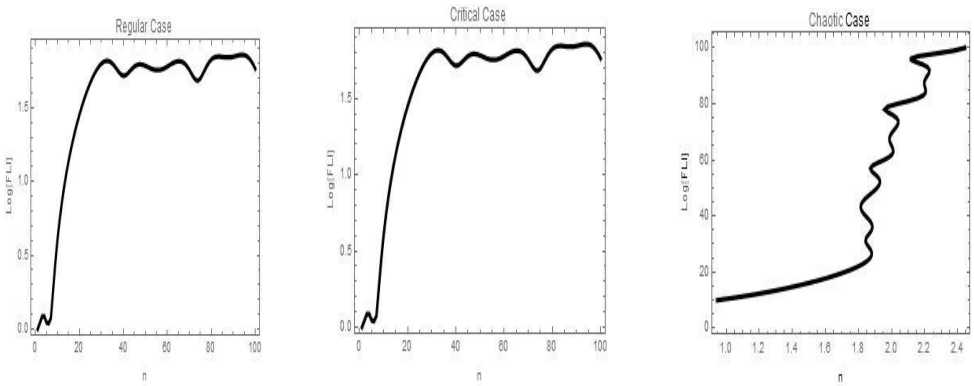


Fig. 8(a). FLI for regular case (b). FLI for critical case (c). FLI for chaotic case

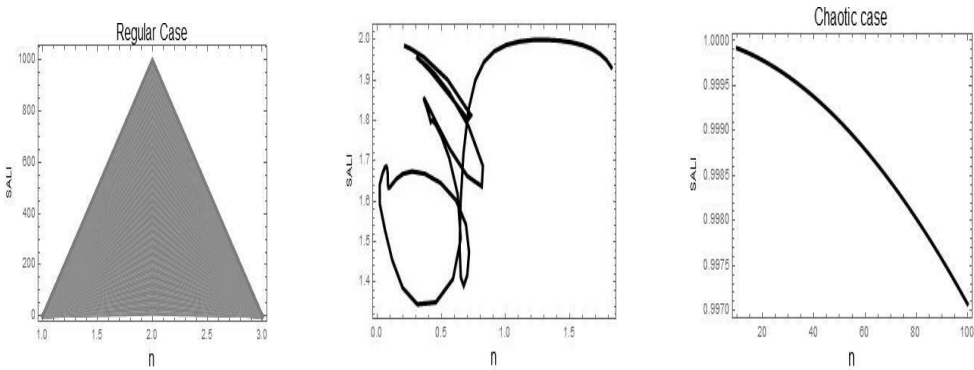


Fig. 9(a). SALI for regular (b). SALI for critical case (c). SALI for chaotic case

5. Conclusion

Magnetic field intensity applied under a specific temperature is thoroughly dependent on the Hartmann number. If Hartmann number is increased or field is varied to higher intensity the chaotic phase of fluid flow

should transit to stable state flow in channelized manner. It is observed that it is used in target specific magnetic drug delivery or CMR applications. It is observed that FLI displays linear increase in case of regular orbits whereas exponential increase for critical behavior and chaotic orbits. DLI indicates a definite pattern in case of regular orbits whereas shows high variation in case of randomness. SALI has a great variation with simultaneous increase and decrease in case of regular case. In case of chaos, SALI values vary differently and after sometime tends to zero. In case of non-uniform deposition, the flow becomes chaotic at extreme temperature and magnetic intensity variations due to the non-uniform choking with narrow spaces available through which some regular flow is still feasible. In case of patients with non-uniform cholesterol deposition, detection of extent of damage with accuracy is easier as curing through normal drug delivery makes possible to flow to the specific target. Thus, the patient with non-uniform cholesterol deposition still has a chance at survival as chaos takes place when exposed to life-threatening situations and due to non-uniformity of deposition narrow in between passages, stable flow occurs.

Acknowledgement: Authors thankful to G.G.S.I.P.U. for research facilities. Authors have no conflict of interest regarding the present study.

References

1. R. Bhardwaj, M. Chawla; Convection Dynamics of Fe_3O_4 nanoparticles in Blood Fluid Flow, *Indian Journal of Industrial and Applied Mathematics*, 9(1) (2018) 23.
2. R. Bhardwaj and A. Bangia; Hybrid Fuzzified-PID controller for non-linear control surfaces for DC motor to improve the efficiency of electric battery driven vehicles, *International Journal of Recent Technology and Engineering (IJRTE)*, 8(3) (2019) 2561-2568.
3. R. Bhardwaj and A. Bangia; Dynamic Indicator for the prediction of Atmospheric Pollutants, *Asian Journal of Water, Environment and Pollution*, 16(4) (2019) 39-50.
4. R. Bhardwaj and A. Bangia; Complexity Dynamics of Meditating Body, *Indian Journal of Industrial and Applied Mathematics*, 7(2) (2016) 106-116.
5. R. Bhardwaj and A. Bangia; Stock Market trend analysis during Demonetization using Soft-Computing techniques. *2018 International Conference on Computing, Power and Communication Technologies (GUCON-2018), IEEE Xplore*, (2019) 696-701.
6. R. Bhardwaj and A. Bangia; Statistical Time series Analysis of Dynamics of HIV, *JNANABHA, Special Issue 48* (2018) 22-27.
7. R. Bhardwaj and A. Bangia; Neuro-Fuzzy Analysis of Demonetization on NSE, *Advances in Intelligent Systems and Computing (AISC)*, (2019) 853-861.

8. R. Bhardwaj and A. Bangia; Dynamical Forensic Inference for Malware in IoT-Based Wireless Transmissions, *Forensic Investigations and Risk Management in Mobile and Wireless Communications*, (2019) 51-79.
9. R. Bhardwaj, A. Kumar, P. Maini, S.C. Kar, L.S. Rathore; Bias free rainfall forecast and temperature trend-based temperature forecast based upon T-170 Model during monsoon season, *Meteorological Applications*, 14(4) (2007) 351.
10. B.Karami, S. Nikoseresht, S. Khodabakhshi; Novel approach to benzimidazoles using Fe₃O₄ nanoparticles as a magnetically recoverable catalyst, *Chin. J. Catal.*, 33 (2012) 298-301.
11. M. Nasr-Esfahani, S.J. Hoseini, M. Montazerzohori, R. Mehrabi, H. Nasrabadi; Magnetic Fe₃O₄ nanoparticles: Efficient and recoverable nanocatalyst for the synthesis of polyhydroquinolines and Hantzsch 1,4-dihydropyridines under solvent-free conditions, *J. Mol. Catal. A: Chemical*, 382 (2014), 99-105.
12. S. Khodabakhshia, M.K. Abbasabadi, S. Heydarianc, S.G. Shirazic, F. Marahel; Fe₃O₄ Nanoparticles as Highly Efficient and Recyclable Catalyst for the Synthesis of 4-Hydroxy-3-[aryloyl(benzamido)methyl]coumarin under Solvent-Free Conditions, *Letters in Organic Chemistry*, 12 (2015).
13. MH Lee, K Cho, AP Shah, P. Biswas; Nanostructured Sorbents for Capture of Cadmium Species in Combustion Environments, *Environ Sci Technology*, 39(21) (2005) 8481-8489.
14. PV Kamat, D. Meisel; Nanoscience opportunities in environmental remediation, *Compt Rend Chim*, 6(8-10) (2003) 999-1007.
15. AG Cuenca, H Jiang, SN Hochwald, M Delano, WG Cance, SR Grobmyer; Emerging implications of nanotechnology on cancer diagnostics and therapeutics, *Cancer*, 107 (2006) 459-466.
16. G Oberdörster, E Oberdörster, J. Oberdörster; Nanotoxicology: an emerging discipline evolving from studies of ultrafine particles, *Environ Health Perspect*, 113 (2005) 823-839.
17. AH Faraji, P. Wipf; Nanoparticles in cellular drug delivery, *Bioorg Chem*, 17 (2009) 2950- 2962.
18. SC McBain, HH Yiu, J. Dobson; Magnetic nanoparticles for gene and drug delivery, *Int J Nanomed*, 3(2008) 169-180.
19. AK Gupta, M. Gupta; Cytotoxicity suppression and cellular uptake enhancement of surface modified magnetic nanoparticles, *Biomater*, 26 (2005) 1565-1573.
20. P. Gould; Nanomagnetism shows in vivo potential, *Nanotoday*, 1 (2006) 34-39.
21. GF Goya, TS Berquo, FC Fonseca, MP. Morales; Static and dynamic magnetic properties of spherical magnetite nanoparticles, *J Appl Phy*, 94 (2003) 3520-3528.
22. A K Gupta, M. Gupta; Synthesis and surface engineering of iron oxide nanoparticles for biomedical applications, *Biomater*, 26 (2005) 3995-4021.
23. M. P. Buman, A.C. King; Exercise as a Treatment to Enhance Sleep, *American Journal of Lifestyle Medicine*, 31(5) (2010) 514.
24. R.V. Buskirk, C. Jeffries; Observation of chaotic dynamics of coupled nonlinear oscillator, *Physical Review*, A31 (1985) 467.

25. C. Froeschle, R. Gonzi, E. Lega; The Fast Lyapunov Indicator: A simple tool to detect weak chaos. Application to the structure of the main asteroidal belt, *Planetary and Space Science*, 45 (1997) 881.